Instructive Nanofibrous Scaffold Comprising Runt-Related Transcription Factor 2 Gene Delivery for Bone Tissue Engineering

Nelson Monteiro,[†,‡] Diana Ribeiro,[†,‡] Albino Martins,[†,‡] Susana Faria,[§] Nuno A. Fonseca,[⊥] João N. Moreira,[⊥] Rui L. Reis,[†,‡] and Nuno M. Neves[†,‡,*]

[†]3B's Research Group—Biomaterials, Biodegradables and Biomimetics, Department of Polymer Engineering, University of Minho, Headquarters of the European Institute of Excellence on Tissue Engineering and Regenerative Medicine, AvePark, Zona Industrial da Gandra S. Cláudio do Barco, 4806-909 Caldas das Taipas, Guimarães, Portugal, [‡]ICVS/3B's, PT Government Associate Laboratory, Braga, Guimarães, Portugal, [§]Department of Mathematics for Science and Technology, Research CMAT, University of Minho, Campus de Azurém, 4800-058 Guimarães, Portugal, and [⊥]Center for Neurosciences and Cell Biology (CNC), Faculty of Pharmacy of the University of Coimbra, 3000 Coimbra, Portugal

ABSTRACT Inducer molecules capable of regulating mesenchymal stem cell differentiation into specific lineages have proven effective in basic science and in preclinical studies. Runt-related transcription factor 2 (RUNX2) is considered to be the central gene involved in the osteoblast phenotype induction, which may be advantageous for inducing bone tissue regeneration. This work envisions the development of a platform for gene delivery, combining liposomes as gene delivery devices, with electrospun nanofiber mesh (NFM) as a tissue engineering scaffold. pDNA-loaded liposomes were immobilized at the surface of functionalized polycaprolactone (PCL) NFM. Human bone-marrow-derived mesenchymal stem cells (hBMSCs) cultured on RUNX2-loaded liposomes immobilized at the surface of electrospun PCL NFM showed enhanced levels of metabolic activity and total protein synthesis. RUNX2-loaded liposomes immobilized at the surface of electrospun PCL NFMs induce a long-term gene expression of eGFP and RUNX2 by cultured hBMSCs. Furthermore, osteogenic differentiation of hBMSCs was also achieved by the overexpression of other osteogenic markers in medium free of osteogenic supplementation. These findings demonstrate that surface immobilization of RUNX2 plasmid onto elestrospun PCL NFM can produce long-term gene expression *in vitro*, which may be employed to enhance the osteoinductive properties of scaffolds used for bone tissue engineering strategies.

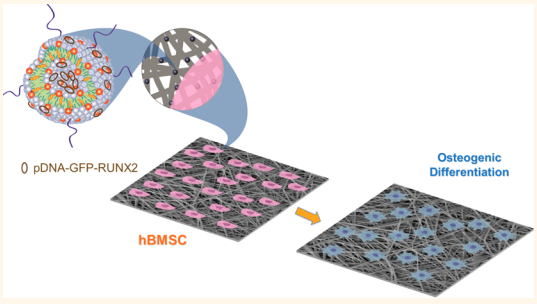

KEYWORDS: liposomes · mesenchymal stem cells · polycaprolactone · gene expression · scaffold · bone tissue engineering

More than 2.2 million bone grafting procedures (*i.e.*, autologous bone graft and banked bone, allografts) take place annually worldwide to ensure adequate bone healing in many skeletal-related problems.[1] However, the harvesting procedure of autologous bone from the iliac crest adds significant morbidity to the surgical procedure, namely, blood loss, postoperative pain, and the risk of infection or fracture.[2] These disadvantages have prompted an ongoing search for alternative methods that would supersede the need for an iliac crest harvest. Furthermore, there is a need for strategies that stimulate bone growth with proper functional properties.[3] Scientific advances in tissue engineering have shown the potential on the combination of a specific progenitor cell population with a scaffold supplied with growth/differentiation factors (GF), to control the spatial and temporal organization of progenitor cell growth, differentiation, and function toward the osteogenic phenotype.[4−6]

The properties of the scaffold can significantly affect the proliferation, differentiation, and matrix deposition by progenitor cells.[5] Fibrous structures mimicking the morphology of the natural extracellular matrix may be useful in bone tissue engineering strategies.[7,8] A nanofibrous scaffold can be used to deliver bioactive agents such

* Address correspondence to nuno@dep.uminho.pt.

Received for review April 16, 2014 and accepted July 21, 2014.

Published online July 21, 2014
10.1021/nn5021049

as GFs and nucleotides.[6,9,10] Gene delivery is a good approach to drive stem cell differentiation.[11] Therefore, the methods of transfection must take into account the negative charge of the cell membrane, the targeting of specific cells, the stability of the pDNA during cytoplasm traveling, the DNA transport into the cell nucleus, and the overexpression of the target gene.[12,13] Viral and nonviral vectors (*i.e.*, liposomes, cationic lipids, polymers, and proteins) are examples of carriers used to transfect cells.[12,14,15] The use of viral vectors leads to higher transgene expression and transduction efficiency and also possesses inherent immunological risks, limited tropism, and size limitations on the inserted transgene.[11] Nonviral delivery systems have been also proposed, but they have comparatively lower efficiency of transfection.[16,17] Cationic lipids have emerged as a choice for gene delivery, and a number of lipids with cationic head groups have been synthesized and evaluated for the transfection of cells.[18] Liposomes, a mixture of cationic lipids and neutral lipids, are another proposed strategy to facilitate the nucleic acid delivery.[19,20] Encapsulation of the pDNA within liposomes can limit the accessibility of DNase and consequently may increase the transfection efficiency. Therefore, the use of gene delivery systems such as liposomes combined with scaffolds may address the issues of toxicity, liposome aggregation, long-term expression, and increased transfection efficiency.[17] Indeed, the delivery of pDNA-loaded liposomes by a biomaterial scaffold may reduce their exposure to immune cells, enhancing the cellular uptake.[17] Moreover, there is the possibility and flexibility of well-controlled and sustained delivery and localized gene expression of tissue inductive factors.[14,17,21]

Adult mesenchymal stem cells (MSCs) are among the safest candidate cell sources for cell-based therapeutics and regenerative medicine. They are diversely distributed *in vivo* and can be directly obtained from individual patients, thereby eliminating the complications associated with the transplantation of allogenic cells. Additionally, their use in research, as well as in therapeutics, is not hindered by ethical considerations unlike embryonic stem cells.[22,23] The self-renewal and the multilineage differentiation capacities of MSCs hold great potential for regenerative medicine strategies.[24,25] MSCs also secrete a large spectrum of bioactive agents such as cytokines and GFs which mediate the cellular activity.[26,27] For bone regeneration, MSCs have been genetically engineered to express bone morphogenic proteins (BMPs) to induce bone healing or bone formation.[28] However, the precise cellular signaling mechanisms by which bone synthesis is controlled within developing osteoblasts and progenitor cells are still to be precisely defined.[29] Gene delivery encoding transcription factors, which drive native protein production, can offer advantages relative to delivering DNA encoding for a specific or to a set of proteins.[30,31] Furthermore, transcription factors that activate the endogenous gene would ensure that expression of all natural splice variants occurs in a coordinated time and sequence. Moreover, the transcription factors may regulate a cascade of multiple different genes, which may be advantageous for tissue regeneration. Runt-related transcription factor 2 (RUNX2) is a member of the RUNX family, and it is considered to be the central control gene within the osteoblastic phenotype.[32] Indeed, mice deficient in RUNX2 failed to form any bone tissue, demonstrating the specific and critical role of this transcription factor in bone development.[33]

On the basis of all those assumptions, in the present work, we developed multifunctionalized electrospun polycaprolactone (PCL) nanofiber meshes (NFMs) with the capacity to be used as a stem cell differentiation inductive structure, through the covalent immobilization of plasmid encoding RUNX2 loaded in the liposomes. Plasmid encoding RUNX2 was loaded into liposomes that were further immobilized at the surface of the electrospun PCL NFMs. The effect of RUNX2-loaded liposomes immobilized at the surface of electrospun PCL NFMs was assessed by quantifying the viability, proliferation, protein synthesis, and differentiation of human bone-marrow-derived mesenchymal stem cells (hBMSCs). We also compared this strategy with RUNX2-loaded liposomes supplemented in the medium, in hBMSCs cultured in tissue culture polystyrene (TCPS) under basal and osteogenic differentiation conditions as experimental controls. We hypothesize that the immobilized liposomes may easily be internalized by the cells that in turn will express high levels of RUNX2 and the consequent physiologic factors relevant for bone homeostasis, leading to a very effective differentiation of hBMSCs.

RESULTS

Development and Characterization. Table 1 presents the liposome formulations used in this study. **F1** was used to optimize the encapsulation of pDNA encoding just GFP (6.6 kb). **F2** was used to encapsulate pDNA encoding GFP-RUNX2 (8.3 kb), for the immobilization at the surface of electrospun PCL NFMs and for visualization of the liposomes by fluorescence microscopy and for further biological assays. Figure 1 shows a scheme of the liposome formulations and the chemical pathway followed for the immobilization of the pDNA-loaded liposomes at the surface of PCL NFM (see Experimental Section).

TABLE 1. Liposome Formulations (Values Expressed as a Molar Ratio)

	DODAP	HSPC	Chol	DSPE-PEG	DSPE-PEG-Mal	PE-Rho
F1	40	27.5	27.5	5		
F2	40	27.5	27.5		5	0.1

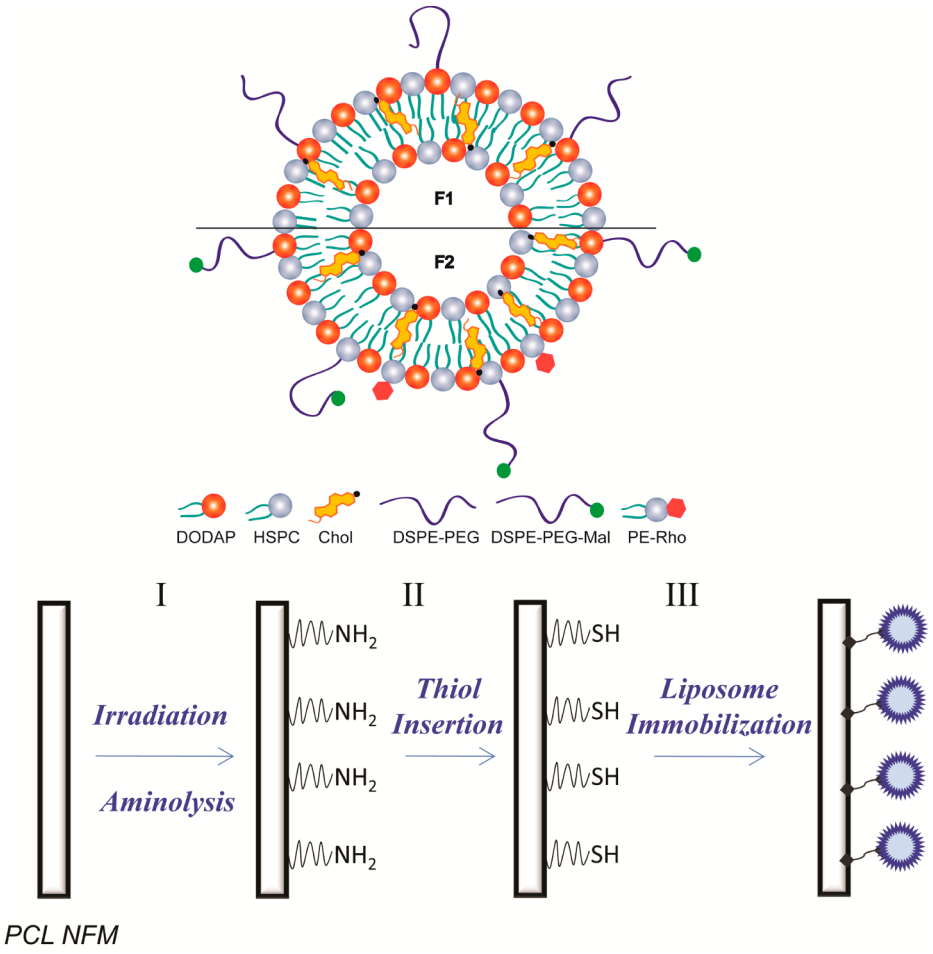

Figure 1. Liposome formulations and chemical pathway for the immobilization of liposomes at the surface of modified PCL NFM. (I) UV-ozone irradiation and aminolysis treatment, (II) primary amine group and 2-iminothiolane reaction (at pH 8), and (III) thiol group and maleimide reaction (at pH 7).

TABLE 2. pDNA Encapsulation Efficiency

pDNA (mg/mL)	ee (%)
0.04	72.16 ± 8.42
0.1	55.18 ± 15.16
0.4	37.93 ± 5.67

TABLE 3. ζ-Potential and Size of pDNA-Loaded Liposome Formulation F1

pDNA (mg/mL)	ζ-potential (mV)	size (nm)
0	8.37 ± 2.93	72.82 ± 4.42
0.04	−5.41 ± 1.15	83.42 ± 14.30
0.1	−6.21 ± 0.39	89.70 ± 20.46
0.4	−10.22 ± 1.40	98.81 ± 19.10

pDNA Encapsulation. As shown in Table 2, the encapsulating efficiency decreases as the pDNA concentration increases. The maximum encapsulation, 72.16 ± 8.42, was reached at 0.04 mg/mL. However, no statistically significant variation was observed between 0.04 and 0.1 mg/mL (55.18 ± 15.16).

pDNA-Loaded Liposome Size and ζ-Potential. Cationic lipid (DODAP), neutral lipids (HSPC and Chol), and PEG lipid (DSPE-PEG) were mixed with plasmid DNA at various concentrations, and some physical properties of the resulting complexes were measured. Table 3 presents the ζ-potential and the particle size of each of the synthesized liposomal formulations. The ζ-potential depends on the charge density at the surface of the liposomes. The ζ-potential was positive for liposomes without pDNA, 8.37 ± 2.93 mV. The ζ-potential of the pDNA-loaded liposomes was negative, and it decreased as the concentration of the pDNA increased. The particle size of the pDNA-loaded liposomes showed a monodisperse distribution, with diameters varying between 72.82 ± 4.42 and 98.81 ± 19.10 nm. The liposome size increased as the concentration of the pDNA was increased.

Stability of the pDNA-Loaded Liposome Suspension. To test the stability of the pDNA-loaded liposomes after preparation, the concentration of pDNA was quantified during 5 h (Figure 2). The condition used to evaluate the stability was 0.4 mg/mL of pDNA loaded into the liposomes (formulation **F1**). The result

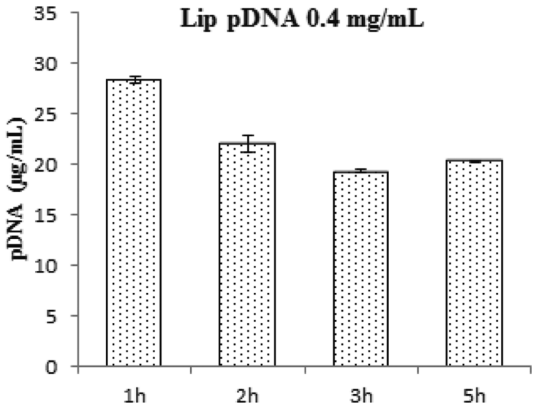

Figure 2. Stability of pDNA-loaded liposomes.

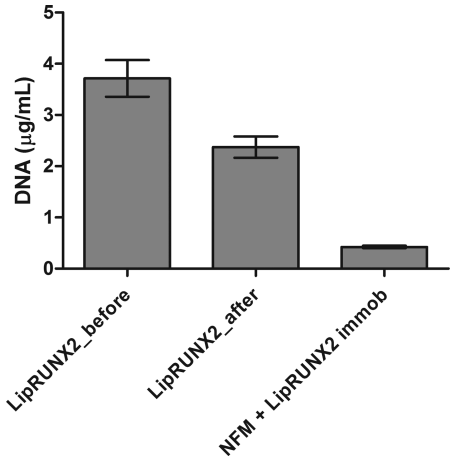

Figure 3. Concentration of pDNA in the liposome solutions before and after immobilization at the surface of electrospun PCL NFMs.

shows that the pDNA concentration decreased after the first hour and remained constant until the 5 h of the study.

Immobilization of the pDNA-Loaded Liposomes to the NFM's Surface. The affinity of the pDNA-loaded liposomes for the SH-functionalized NFMs was studied using the formulation **F2** and the pDNA concentration of 0.1 mg/mL. For that, after pDNA-loaded liposome immobilization, the concentration of pDNA was determined (Figure 3). The results show that the concentration of the pDNA in the liposome solution decreased after immobilization, which confirms the binding of pDNA-loaded liposomes at the NFM's surface. Specifically, approximately 10% of the pDNA-loaded liposomes are immobilized at the surface of electrospun PCL NFMs.

Figure 4 presents the SEM, fluorescence micrographs of binding sites, and pDNA-loaded liposomes immobilized at the surface of electrospun PCL NFMs. In the SEM micrograph (Figure 4A), it is observed that the integrity of the fibers at the surface is significantly affected by the UV-ozone irradiation and aminolysis.[34] From the SEM micrographs (Figure 4B), the presence of one liposome (diameter of 118 nm) immobilized at the surface of the NFM is observed. The observed uniform distribution of the binding sites and pDNA-loaded liposomes immobilized at the surface of electrospun PCL NFMs (Figure 4C,D) demonstrates that the SH functionalization and the liposome immobilization steps were successful.

Biological Activity. *Cell Proliferation and Viability Assessment.* Suspension liposomal RUNX2 delivery and scaffold-mediated RUNX2 delivery conditions were assessed by substrate (*i.e.*, *TCPS* or *NFM*) and by culture media condition (*i.e.*, *Basal* or *Osteo*). The different culture conditions *NFM_Basal*, *NFM_Osteo*, and *NFM+ LipRUNX2* did not induce significant changes over hBMSC's proliferation (*i.e.*, DNA concentration) over the different culture times, that is, in the seventh (p = 0.015), the 14th (p = 0.680), and the 21st day (p = 0.989) (Figure 5). While not statistically significant, *NFM+ LipRUNX2* tendentially displayed a higher DNA concentration when compared to the NFM controls. Likewise, we found no statistically significant differences between *TCPS_Basal*, *TCPS_Osteo*, and *TCPS_LipRUNX2(susp)* in terms of DNA concentration in the seventh day (p = 0.043) and in the 21st day (p = 0.233). Although, in the 14th day, *TCPS_Basal* displayed a significantly higher DNA concentration than *TCPS_Osteo* and *TCPS_LipRUNX2(susp)* ($p < 0.001$). Finally, hBMSCs cultured in NFMs show lower DNA amounts compared to similar conditions in TCPS culture (Mann−Whitney U test, $p < 0.001$). We may speculate that this decrease in DNA proliferation is associated with an increase in the efficacy of cell differentiation that usually leads to lower mitogenic activity of the cells.

Similar to the analysis of hBMSCs' proliferation along the time course of the experiment, the viability of those cells, cultured in TCPS or NFM, under basal or osteogenic medium and in the presence of RUNX2-loaded liposomes, either in suspension or immobilized at the surface of electrospun NFMs, did not induce significant changes over hBMSCs' viability (Figure 6). One exception was found for the seventh day, where *TCPS_Osteo* displayed a significantly lower values than *TCPS_LipRUNX2(susp)* ($p < 0.001$). Conversely to the proliferation results, a higher viability was verified in all NFM culture conditions compared to all the TCPS culture conditions, for all time culture periods ($p < 0.001$).

Concerning the hBMSCs' total protein synthesis (Figure 7), we found no significant differences between RUNX2-stimulated cells and the correspondent controls, either cultured on TCPS or NFMs. Even though, on the 14th day, *TCPS_Osteo* displayed a significantly lower protein concentration than *TCPS_LipRUNX2(susp)* ($p < 0.01$). On the 21st day, *TCPS_Osteo* displayed a significantly higher protein concentration ($p < 0.001$).

Following the previous results on hBMSCs' metabolic activity, there is an evident increase in the total protein synthesis per cell for all the NFM culture

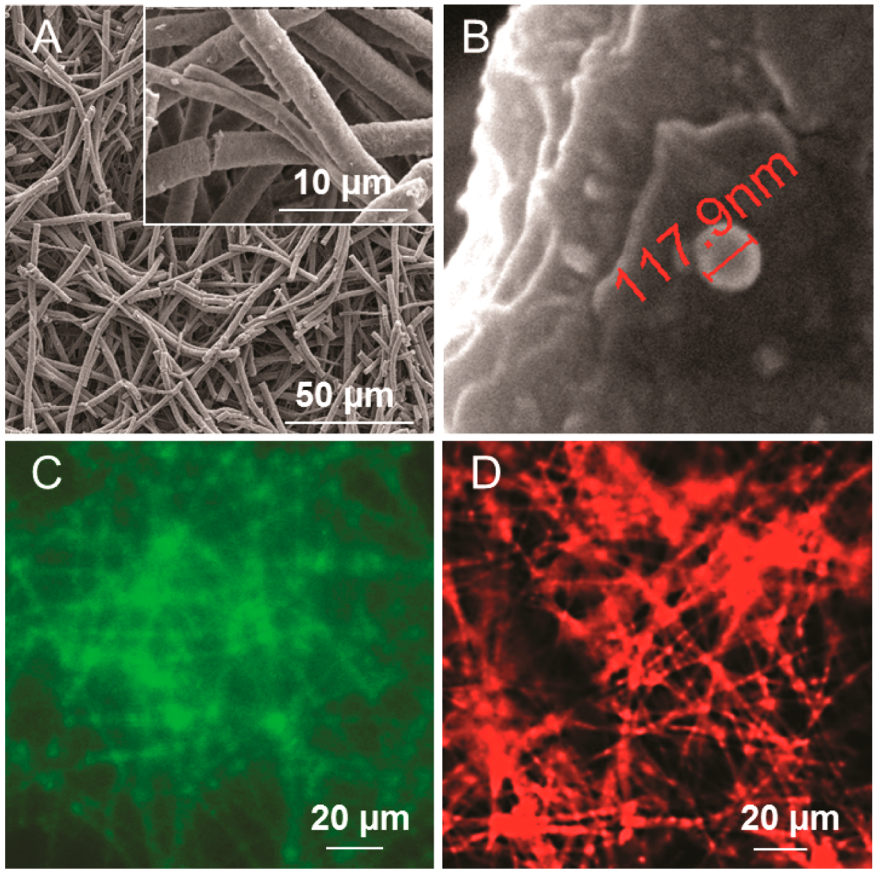

Figure 4. SEM and fluorescence micrographs: (A) morphology of functionalized PCL NFMs (4 min UV-ozone irradiation and 1 h aminolysis); (B) detail of a liposome (F2) immobilized at the surface of functionalized NFMs (t = 4 min); (C) SH-functionalized NFM reacted with BODIPY; (D) fluorescence micrograph of PE-Rho marked liposomes immobilized at the surface of SH-functionalized NFM.

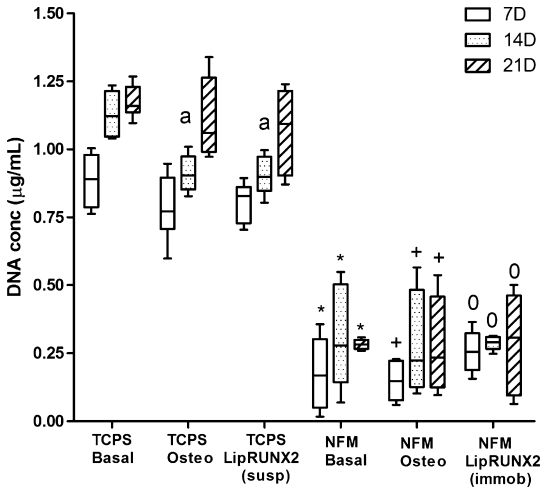

Figure 5. Box plot of hBMSC proliferation (DNA concentration (μg/mL)). When cultured on TCPS or NFM, under basal or osteo medium and in the presence of RUNX2-loaded liposomes, either in suspension or immobilized at the surface of electrospun NFMs. A set of three time points was established: 7, 14, and 21 days of culture; "a" denotes significant differences compared to *TCPS_Basal*. Nonparametric way of a Mann−Whitney U-test: *p < 0.01 *TCPS_Basal vs NFM_Basal*, ^{+}p < 0.01 *TCPS_Osteo vs NFM_Osteo*, and "0" p < 0.01 *TCPS_LipRUNX2(susp) vs NFM+LipRUNX2*.

conditions when compared with the TCPS controls. In fact, all the NFM culture conditions displayed significantly higher protein concentration/cell than all TCPS culture conditions, for all time points (p < 0.001).

Long-Term Expression Profile of pDNA. The major advantage of the instructive scaffolds for gene delivery, such as scaffolds as gene carrier and support device for cell culture, is the possibility and flexibility of a sustained gene delivery in the neighborhood of culturing cells. In fact, in Figure 8, it is demonstrated that RUNX2-loaded liposomes immobilized at the surface of electrospun NFMs showed a long-term gene expression of eGFP (present in the plasmid pCMV6::eGFP-RUNX2) by adherent and culturing hBMSCs. Comparably, hBMSCs cultured with RUNX2-loaded liposomes in suspension, at the same concentration as the RUNX2-loaded liposomes immobilized at the surface of electrospun NFMs, express approximately 30 000 times less eGFP by the first time point with further zero decrease. It is also notable that, along the time course of the experiment, the eGFP was consistently expressed by the cells cultured in the liposome-immobilized NFMs.

Genotypic Expression of Osteoblastic Markers. A quantification of some bone-specific gene expression

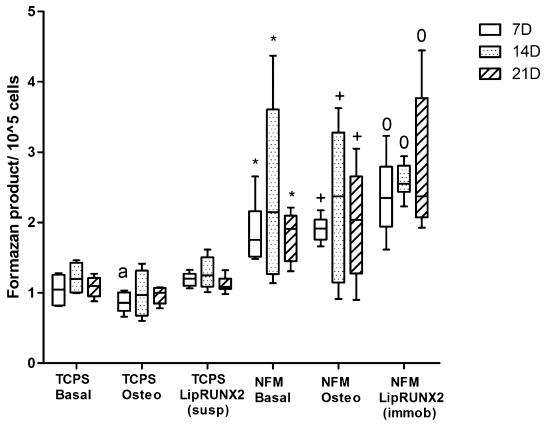

Figure 6. Box plot of hBMSCs' metabolic activity (normalized by the cell number) cultured on TCPS or NFM, under basal or osteo medium and in the presence of RUNX2-loaded liposomes, either in suspension or immobilized at the surface of electrospun NFMs. A set of three time points was established: 7, 14, and 21 days of culture; "a" denotes significant differences compared to *TCPS_LipRUNX2(susp)*. Nonparametric way of a Mann−Whitney U-test: *$p < 0.01$ *TCPS_Basal vs NFM_Basal*, $^{+}p < 0.01$ *TCPS_Osteo vs NFM_Osteo*, and "0" $p < 0.01$ *TCPS_LipRUNX2(susp) vs NFM+LipRUNX2*.

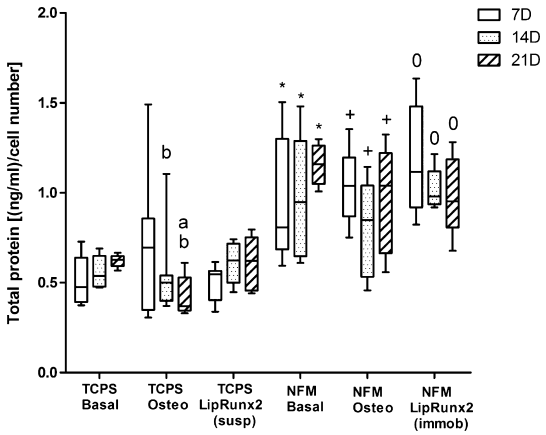

Figure 7. Box plot of hBMSCs protein synthesis (ng/mL) (normalized by the cell number) cultured on TCPS or NFM, under basal or osteo media and in the presence of RUNX2-loaded liposomes, either in suspension or immobilized at the surface of electrospun NFMs. A set of three time points was established: 7, 14, and 21 days of culture; "a" denotes significant differences compared to *TCPS_Basal*; "b" denotes significant differences compared to *TCPS_LipRUNX2-(susp)*. Data were analyzed by nonparametric way of a Mann−Whitney U-test: *$p < 0.01$ *TCPS_Basal vs NFM_Basal*, $^{+}p < 0.01$ *TCPS_Osteo vs NFM_Osteo*, and "0" $p < 0.01$ *TCPS_LipRUNX2(susp) vs NFM+LipRUNX2*.

was performed to ascertain the differentiation level of the hBMSCs subject to the stimulus of RUNX2-loaded liposomes in suspension or immobilized at the surface of electrospun NFMs (Figure 9). The hBMSC culture on the RUNX2-loaded liposomes immobilized at the surface of electrospun NFMs intensively overexpressed the RUNX2 gene overtime, as previously indirectly analyzed by the expression of eGFP (Figure 8). In fact, *NFM+LipRUNX2* displayed a significantly higher

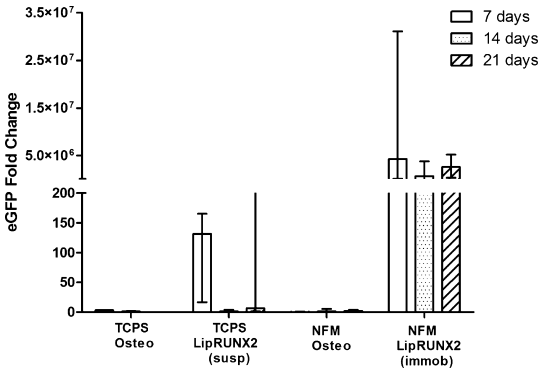

Figure 8. Relative expression of eGFP present in the RUNX2 plasmid by hBMSCs cultured on TCPS or NFM, under basal or osteo medium and in the presence of RUNX2-loaded liposomes, either in suspension or immobilized at the surface of electrospun NFMs. A set of three time points was established: 7, 14, and 21 days of culture. The expression was normalized against the housekeeping gene *GAPDH* and the basal condition as calibrator. The $2^{-\Delta\Delta CT}$ method (Livak method) was used to calculate the fold changes.

RUNX2 gene expression than *NFM_Osteo* on the seventh, 14th, and the 21st day ($p = 0.002$). In contrast to the immobilized liposomes, the RUNX2-loaded liposomes in suspension (*i.e.*, *TCPS_LipRUNX2*) did not reveal any significant difference compared to the control condition of *TCPS_Osteo*. While no significant differences were found for the remaining osteogenic markers, a slight overexpression of the osteocalcin and osteopontin genes is observed for the *NFM+LipRUNX2*, especially on the earlier time point ($p = 0.029$).

Alkaline Phosphatase Activity Quantification. To conclude about the differentiated phenotype of culturing hBMSCs, alkaline phosphatase (ALP) activity was quantified by using the *p*-nitrophenol assay (Figure 10). hBMSCs cultured on TCPS under osteogenic conditions produced significantly higher quantities of ALP than the control condition in basal media (*i.e.*, *TCPS_Basal*) and the RUNX2 stimulus condition in suspension (*i.e.*, *TCPS_LipRUNX2(susp)*) for the 14th and the 21st days of culture ($p < 0.001$). For the NFM culture conditions, at the seventh day, *NFM_Basal* displayed a significantly lower ALP activity than *NFM_Osteo* and *NFM+LipRUNX2* ($p < 0.001$). Moreover, the *NFM_Osteo* condition displayed a significantly higher ALP activity than the *NFM+LipRUNX2* condition ($p < 0.001$) for the seventh and the 14th days of hBMSC culture. Although the ALP activity of hBMSCs cultured on *NFM_Basal* and *NFM_Osteo* increase significantly over the different culturing days ($p < 0.001$), *NFM+LipRUNX2* only displayed a significantly higher ALP activity at the 21st day ($p < 0.001$). Furthermore, hBMSCs cultured on *TCPS_LipRUNX2(susp)* produced negligible quantities of ALP, comparable to *TCPS_Basal*.

DISCUSSION

Liposomes have been used as carriers of nucleic acids (pDNA, antisense oligonucleotides, or small interfering

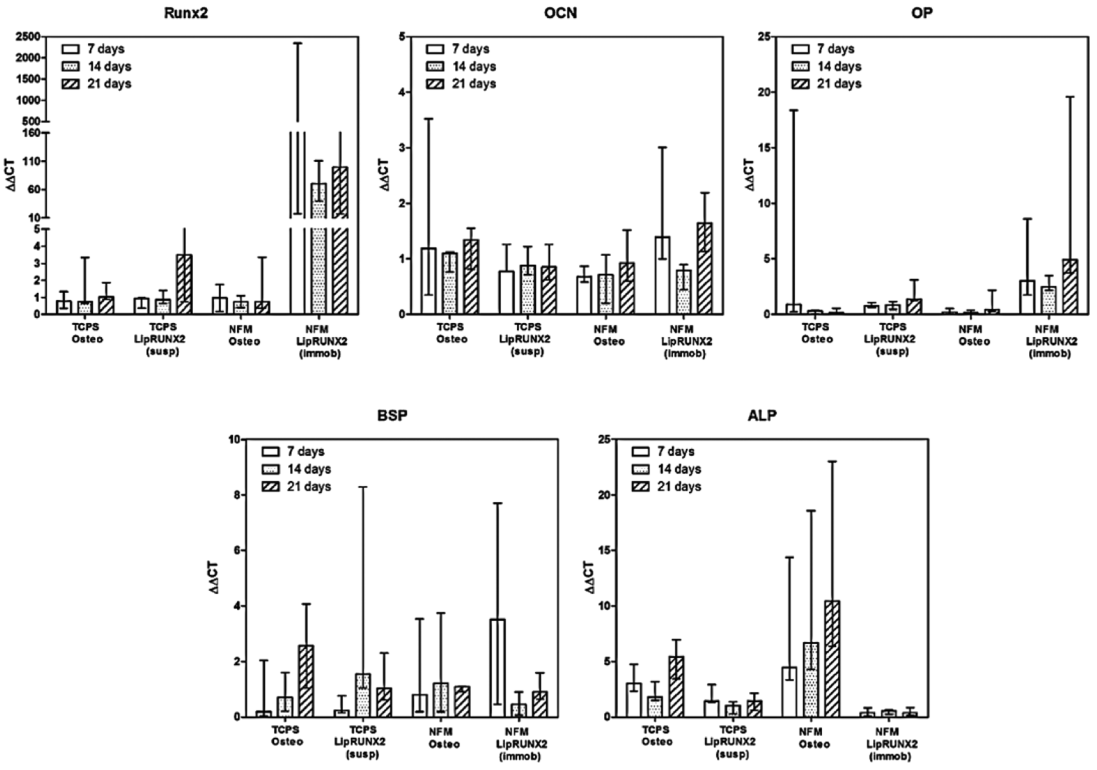

Figure 9. Bar plot of the relative expression of osteogenic markers by hBMSCs cultured on TCPS or NFM, under basal or osteo medium and in the presence of RUNX2-loaded liposomes, either in suspension or immobilized at the surface of electrospun NFMs. A set of three time points was established: 7, 14, and 21 days of culture. The expression was normalized against the housekeeping gene *GAPDH* and the basal culture condition as calibrator. The $2^{-\Delta\Delta CT}$ method (Livak method) was used to calculate the fold changes on osteoblastic gene expression.

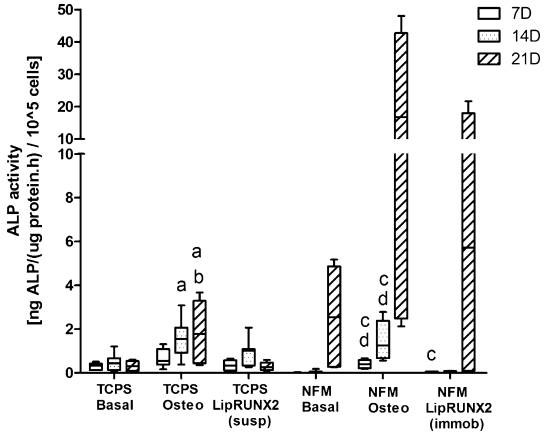

Figure 10. Box plot of the ALP activity (nmol ALP/(μg protein $\times$ h) (normalized by the cell number) cultured on TCPS or NFM, under basal or osteo medium and in the presence of RUNX2-loaded liposomes, either in suspension or immobilized at the surface of electrospun NFMs. A set of three time points was established: 7, 14, and 21 days of culture. Data were analyzed by nonparametric way of a Kruskal–Wallis test followed by Tukey's HSD test: the three TCPSs were compared, and the three NFMs were compared: "a" denotes significant differences compared to *TCPS_Basal*, "b" denotes significant differences compared to *TCPS_LipRUNX2(susp)*, "c" denotes significant differences compared to *NFM_Basal*, and "d" denotes significant differences compared to *NFM+LipRUNX2*.

RNA (siRNA)).[13,19,35] This lipoplex has been used to transfect cells *in vitro* and *in vivo* in order to promote the expression of defined genes.[17,36] Ideally, a gene delivery system should be able to encapsulate the nucleic acid, to protect it from the physiological degradation during the traveling across the intracellular space and to release the nucleic acid into the nucleus inside the cell.[19] The tissue engineering approach involves a biomaterial scaffold, which mimics the natural extracellular matrix, committed cells, and specific bioactive agents. Gene delivery may provide an alternative approach by which gene-stimulated cells may trigger the production of bioactive signals in an *in vivo*-like fashion enhancing the efficacy of this strategy.

Development and Characterization. A variety of lipid compositions has been used to produce pDNA-loaded liposomes using various methods.[37] However, those methods have limitations such as the liposome size, low encapsulation efficiency, being a time-consuming method, formation of the liposomes before encapsulation, difficulties in scale-up, and short *in vivo* circulation times. One way to encapsulate pDNA inside the inner core of the liposome is using the ethanol injection method by the optimization of the concentration of ethanol, buffer pH, and ionic strength.[37] In this method, the ethanol makes the lipid membrane susceptible to structural rearrangements, leading to an efficient formation of a lipid bilayer encapsulating the pDNA particles and facilitating liposome formation.[37]

Also, the incorporation of PEG–lipid elements into the membrane helps the liposome formation.[19] Moreover, the second dilution step, by increasing the pH and salt concentration, also improves the pDNA encapsulation. The effect of increasing the pH is thought to be a result of the net charge on the lipid in the pDNA-loaded liposome. The effect of increasing the NaCl concentration is related to the structure adopted by the pDNA in the presence of NaCl.[38] The increase in the efficiency of pDNA encapsulation may result from a more contact structure of the pDNA, increasing the charge density and providing more efficient association with lipid bilayer fragments that assemble to become liposomes containing pDNA.[37]

In this work, we succeeded in preparing pDNA (6.6 and 8.3 kb)-loaded liposomes using a stepwise ethanol injection method and their immobilization at the surface of electrospun PCL NFMs. The liposomal formulations were composed mainly by the positively charged lipid DODAP, the neutral lipid HSPC, the cholesterol, and the DSPE-PEG to improve the stability of the liposomes. The results showed that the encapsulation efficiency decreased as the pDNA (6.6 kb) concentration increased. This indicates that, at 0.04 mg/mL pDNA, a maximum of the encapsulation efficiency was achieved. It was already described by others that the large molecular weight of pDNA may make its encapsulation within the inner core of liposomes difficult.[19] However, and in accordance with our results, pDNAs with sizes varying from 4.4 to 15 kb have been successfully encapsulated using a lipid composition containing a range of tertiary and quaternary cationic lipids, including DODAP, DOTAP, and DODAC.[37,39] Furthermore, the ethanol injection method allows encapsulation efficiencies of up to 70%,[37,40] which may be attributed to the electrostatic adsorption of pDNA to the inner leaflet of the cationic liposome membrane.[19]

The ζ-potential results show that the liposome surface was more negative as the pDNA concentration was increased. Likewise, the liposome's size increased as the pDNA concentration was increased. On the basis of these results, we can speculate that the pDNA may be partially encapsulated inside the inner compartment of the liposomes, but also some parts of it may show up at the liposomes' surface. Therefore, decreasing the pDNA concentration, less pDNA will be exposed at the surface of the liposomes and, consequently, the ζ-potential will also decrease. Indeed, cationic lipids interact with nucleic acids by electrostatic interactions between the positively charged lipids and the negatively charged nucleic acids to form lipoplexes.[41]

The SEM micrographs (Figure 4A) shows that the UV-ozone irradiation and aminolysis have a significant effect on the integrity of the electrospun PCL NFM causing shortening of the fibers. The damage to the nanofibers is mainly due to the aminolysis reaction, as it was previously reported.[34] However, the morphology of the nanofibers present in the bulk of the mesh underneath the surface is not significantly affected by the irradiation or by the chemical treatment.[34] A BODIPY fluorescent dye was covalently bound to the SH groups present at the surface of electrospun NFMs. Figure 4C shows the homogeneous distribution of SH functionalization at the surface of the irradiated and chemically functionalized electrospun NFMs. The DSPE-PEG-Mal lipids comprising the outer layer of the liposomes allow binding to the SH groups grafted at the surface of electrospun NFMs.[34] Specifically, the maleimide group (Mal) reacts with SH groups when the pH is between 6.5 and 7.5, forming a nonreversible and stable thioether linkage. The efficiency of surface-bonded PEG chains is explained by the steric repulsive barrier around the liposomes provided by the covalently bonded PEG.[42] Based on those statements, our result showed that approximately 10% of the pDNA-loaded liposomes are immobilized at the surface of SH-functionalized electrospun NFM. This means that the SH groups were saturated, and some of the liposomes were not covalently linked to the electrospun nanofiber surface. Thus, the amount of liposomes immobilized is specifically controlled by the amount of SH groups available at the nanofibers' surface, with the remaining liposomes removed by the washing step. The spatial distribution of the liposomes at the surface of electrospun NFMs was evaluated by fluorescence microscopy emitted by the rhodamine dye (Figure 4D). This analysis showed that the immobilization at the surface of pDNA-loaded liposomes was successful and evenly distributed throughout the surface of the NFM.

Biological Activity. Transfection of cells, either using viral or nonviral nanoparticles *in vitro*, can be performed in suspension (also referred to as forward transfection) and/or immobilized at the substrate such as a scaffold (also referred to as reverse transfection).[43] In the transfection by immobilization of nanoparticles at the surface of the scaffold, the cells are seeded on top of the nanoparticles. Conversely, in transfection of the suspension, the nanoparticles are added to previously seeded cells. The combination of gene therapy with scaffolds may be a solution to avoid nanoparticle dispersion, to address the issues of toxicity and aggregation, and to reduce administration dose, long-term expression, and increased transfection efficiency.[17,43,44] It is known that adult stem cells are more difficult to transfect, and an effective gene delivery system is needed.[45,46] Having this in mind, we performed an exhaustive biological characterization comparing the efficacy of scaffold-mediated liposome gene delivery and suspension liposome delivery.

Our biological data showed that RUNX2-loaded liposomes in suspension or immobilized at the surface of electrospun PCL NFMs exhibited no cytotoxicity to

hBMSCs; the values of DNA and of metabolic activity are comparable with and without liposomes. Figure 5 shows that hBMSCs cultured in NFMs had a low DNA amount when compared to the TCPS. We can speculate that this decrease in proliferation is related to an earlier commitment of the hBMSCs into the osteogenic lineage, led by the 3D environment of nanofibrous meshes but not achieved in the 2D environment of TCPS. Our results demonstrate that the hBMSCs cultured on the electrospun NFMs enhanced the level of metabolic activity and the total protein synthesis per cell (Figures 6 and 7). Moreover, RUNX2-loaded liposomes immobilized at the surface of electrospun NFMs showed a long-term gene expression of eGFP by hBMSCs (Figure 8). This result was also confirmed by the significant overexpression of RUNX2 gene overtime (Figure 9). Altogether, these results highlight the intrinsic benefits offered by the immobilization of liposomes at the surface of a nanofibrous scaffold as a drug delivery vehicle and support for cell growth. hBMSCs can interact directly with the RUNX2-loaded liposomes and internalize them, inducing an earlier achievement of the osteogenic phenotype. Indeed, our results indicated that RUNX2 overexpression in hBMSCs leads to the induction of features consistent with an osteoblast genotype, namely, the osteocalcin and osteopontin gene expression, as well as demonstrated higher ALP activity (Figure 10). The proposed strategy allows overcoming the short-term effect of gene expression following liposomal delivery and the need for repetitive administrations of the liposomal suspensions.

There are several reports in the literature using viral and nonviral nanoparticles for gene delivery.[44,46,47] As an example of viral gene delivery system, Yang *et al.*[47] studied the effect of adenovirus expressing RUNX2 (AdRUNX2) and BMP2 (AdBMP2) in the pluripotent C3H10T1/2 cell line. Immobilization of nanoparticle gene delivery can enhance gene transfer by increasing the concentration of DNA in the cellular microenvironment.[46] The reverse transfection enhanced and prolonged gene expression in MSCs when compared with the conventional method.[48] Furthermore, it was possible to transfect the MSCs in the presence of serum, which overcomes the effects of poor culture media and lowered cytotoxicity.[48] In another study, adenovirus expressing RUNX2 (AdRUNX2) was conjugated to the PCL surface through antibody−antigen interaction. The culture substrate enhanced the *in vitro* osteogenic differentiation of BMSCs.[44] ALP activity was investigated in the AdRUNX2 immobilized PCL surface, showing an increase from seventh to 10th day.[44] In the present study, ALP gene expression was negligible for all RUNX2 stimulus conditions. *NFM+LipRUNX2* displayed high levels of ALP activity on the 21st day, at levels equivalent to those observed on standard osteogenic culture conditions. ALP plays a crucial role in the initiation of mineralization, though is not required for the continuation of mineralization of bone nodules.[49] Further, the levels of alkaline phosphatase activity are not proportional to the observed mineralization levels,[50] and mineralization formed during *in vitro* osteogenesis studies is rarely achieved, and subsequently are characterized with low levels of detail.

The overexpression of RUNX2 recapitulates a serial of osteogenic regulatory events, which triggers the sequential and temporal expression of osteogenic factors, leading to the accumulation of ALP enzyme at later *in vitro* culture times. Some issues have been raised in the literature related to the temporal relationship between the expression of RUNX2 and other osteoblast markers.[51,52] Han *et al.*[53] reported AdRUNX2-modified rabbit adipose-derived stem cells seeded onto polylactic acid/polycaprolactone (PLA/PCL) scaffolds to create a gene-modified tissue-engineered bone. The modified scaffold combined with a vascular bundle was used to repair a rabbit radial defect *in vivo*. It was demonstrated that RUNX2 regulates the expression of VEGF, cell migration, and vascular invasion in bone.[53] It has also described the regulatory effect of RUNX2 over the *Osterix* expression at an early stage of the osteoblastic differentiation[52] and on the upregulation of the *Osteocalcin* promoter activity in an osteosarcoma cell line.[54]

The transfection of cells by immobilization of a defined gene delivery system at the surface of a scaffold may be effective for *in vivo* applications.[53] The result of the present study indicates that the RUNX2-loaded liposomes immobilized at the surface of electrospun PCL NFMs cultured with hBMSCs express high levels of osteoblastic markers. Therefore, this multifunctionalized nanostructured system may be used to regulate the osteogenic differentiation *in vivo*. Further studies will be required to confirm this strategy in bone tissue engineering approaches in animal models, but the efficacy of this strategy *in vitro* shows already that this method may be very effective as a highly functional cell carrier for bone therapies.

CONCLUSIONS

The present work enables concluding that PCL NFM can be functionalized to immobilize liposomes. We also demonstrate that we can load the liposomes with pDNA. The pDNA-immobilized liposomes are effective in differentiating hBMSCs. hBMSCs cultured in the RUNX2-loaded liposome-immobilized electrospun NFMs presented enhanced levels of metabolic activity and total protein synthesis per cell. Moreover, RUNX2-loaded liposomes immobilized at the surface of electrospun NFMs showed a long-term gene expression of eGFP and RUNX2, as well as an early onset of other osteoblastic marker expression when compared with RUNX2-loaded liposomes supplied in suspension.

Concluding, the proposed multifunctionalized system can act, simultaneously, as a gene delivery device and a tissue engineering scaffold. It can be designed to operate as a synthetic support for MSC growth and differentiation, allowing one to maximize spatially the delivery of a defined gene stimulus, by providing high contact area between the hBMSCs and the immobilized pDNA.

EXPERIMENTAL SECTION

Production and Characterization. *Materials.* Polycaprolactone (M_w 80 000), 1,6-hexamethylenediamine (HMD), isopropyl alcohol (IPA), 4-(dimethylamino)pyridine (DMAP), *N*,*N*-dimethylformamide, chloroform, ammonium molybdate, fiske-subbarow reducer, Ellmans reagent (DTNB), 2-iminothiolane (2IT), sepharose CL4B, hepes buffer solution (HBS), citric acid, and sodium citrate were reagent grade and purchased from Sigma-Aldrich. The lipids L-α-phosphatidylethanolamine-*N*-(lissamine rhodamine B sulfonyl) (ammonium salt) (egg-transphosphatidylated, chicken) (PE-Rho), 1,2-distearoyl-*sn*-glycero-3-phosphoethanolamine-*N*-[methoxy(polyethylene glycol)-2000] (ammonium salt) (DSPE-PEG), cholesterol (ovine wool, >98%) (Chol), L-α-phosphatidylcholine, hydrogenated (soy) (HSPC), 1,2-distearoyl-*sn*-glycero-3-phosphoethanolamine-*N*-[maleimide(polyethylene glycol)-2000] (DSPE-PEG-Mal), and 1,2-dioleoyl-3-dimethylammonium propane (DODAP) were purchased from Avanti Polar Lipids. All the materials were used as received.

Preparation of Electrospun PCL NFM. The production of electrospun PCL NFMs was performed as described in detail elsewhere.[6] Briefly, a polymeric solution of 17% w/v PCL in chloroform and *N*,*N*-dimethylformamide (7:3 volume ratio) was electrospun at 8−10 kV, using a needle-to-ground collector distance of 20 cm and a flow rate of 1.0 mL/h. The NFMs were collected on a flat tracing foil, and the solvents were evaporated under vacuum. The electrospun NFMs were cut in 1 cm^2 squares for further testing.

Surface Functionalization of NFMs. The surface functionalization of the PCL NFMs was performed as described elsewhere.[34] Figure 1 shows a scheme of the chemical pathway followed for the immobilization of the pDNA-loaded liposomes at the surface of PCL NFM. The electrospun PCL NFM surfaces were activated by UV-ozone irradiation by using the ProCleaner system, which emits UV light at 254 nm (intensity 10−13 mW/cm^2) and 185 nm (10% intensity of the 254 nm line) (Figure 1I). The same treatment time (*i.e.*, 4 min) was applied to both sides of the electrospun PCL NFMs. The activated surfaces of NFMs were immersed in 1 M HMD solution and incubated for 1 h at 37 °C in order to graft amine groups onto the NFM surfaces. Afterward, SH groups were linked at the surface of the NFMs (Figure 1II) through the reaction of the aminated surfaces with 20 mM 2IT solution (0.1 mM PBS at pH 8, 20 mM DMAP) for 1 h at 37 °C. The amount of SH groups grafted onto the NFM surfaces was quantified using the Ellman's reagent method.[55] Briefly, the samples were immersed in 0.1 mM DTNB solution (in 0.1 mM PBS at pH 7.27) and incubated for 1 h at 37 °C. Thereafter, the UV absorbance of the supernatant (in triplicate) at 412 nm (Synergie HT) was used to quantify the SH groups, using the DTNB solution as blank for 3 h. For the calculation of the NTB^{-2} molar absorption coefficient, the value of 14 151 M^{-1} cm^{-1} was used. The morphologies of the activated and chemically functionalized NFMs were characterized by scanning electronic microscopy (SEM; NanoSEM, Nova 200). Prior to this analysis, the samples were coated with gold/palladium using a Cressington sputter coater 208 HR device. To assess the distribution of SH groups at the surface of electrospun NFMs, three samples of SH-functionalized PCL NFMs were immersed in a preprepared fluorescent BODIPY (493/503 FL *N*-(2-aminoethyl)maleimide) solution (0.4 mM BODIPY in PBS at pH 7). The SH-functionalized PCL NFMs were incubated for 4 h at room temperature. As negative control, untreated samples were immersed in an equivalent solution. Afterward, both types of NFMs were washed three times for 5 min with Tween 20 washing solution (0.5% (v/v) Tween 20 and phosphate buffer at pH 7) by gentle shaking. As the BODIPY is sensitive to light, all the steps were carried out under light protection. Binding of fluorescent dye to the NFMs was further analyzed by fluorescence microscopy (AXIOIMAGE RZ1M, ZEISS, Germany).

pDNA Encoding RUNX2. The fusion of RUNX2 gene sequence (NM_001024630.2, 8.3 kb) at the turboGFP C-terminus coding sequence was engineered using the plasmid pCMV6-AN-GFP (PS100019; OriGene company, USA; 6.6 kb). The backbone vector (CMV::AN-GFP) carries the CMV promoter, the hGH (human growth hormone) polyA signal located downstream of the insert, the ColE1 ori for bacterial origin of replication, the SV40 ori for mammalian cells replication, and an ampicillin resistance marker. Chemically competent *Escherichia coli* DH5α cells, grown in Luria-Bertani medium supplemented with 150 μg/mL ampicillin, were subjected to transformations using the heat shock method. ORFs cloned in this vector were expressed in mammalian cells as a tagged protein with an N-terminal tGFP tag. TurboGFP (excitation/emission max = 482/502 nm) was mainly intended for fast appearance of bright fluorescence. Preparation of pDNA for transfection (*i.e.*, ultrapure and highly concentrated) was performed using the Plasmid Midi kit (Qiagen), according to the manufacturer's instructions. pDNA preps isolated in such a way typically render a yield of ∼2.0−4.0 μg/μL. The pDNA constructs were confirmed by restriction analysis.

Preparation and Characterization of RUNX2-Loaded Liposomes. Table 1 presents the liposome formulations used in this study. **F1** was used to optimize the encapsulation of pDNA encoding just GFP (6.6 kb). **F2** was used to encapsulate pDNA encoding GFP and GFP-RUNX2 (8.3 kb) for the immobilization at the surface of electrospun PCL NFMs and for visualization of the liposomes by fluorescence microscopy and for further biological assays. The production of pDNA-loaded liposomes was performed by the ethanol injection method.[37,40] This process requires the use of up to 40% ethanol (v/v) and an initial acidic pH where the DODAP is positively charged.

Lipids (10 mg/mL total lipid) were dissolved in 0.4 mL of 100% ethanol. pDNA was diluted in 0.3 mL of 20 mM citrate buffer solution pH 4.0 in a separate tube to achieve the concentrations of 0.04, 0.1, and 0.4 mg/mL. The pDNA and lipid solutions were warmed for 2−3 min at 65 °C, and the lipids were added slowly to the pDNA solution while mixing constantly. Afterward, 0.3 mL of 300 mM NaCl and 20 mM of citrate buffer solution at pH 6 was slowly added to the liposome solution and warmed at 65 °C. The liposomal suspension was extruded at $T > T_c$ and through a porous polycarbonate membrane (pore size of 100 nm) held between two tight syringes, which were used to force the solution back and forth (21 times). Non-encapsulated pDNA was removed from the solution by column chromatography (Sepharose CL4B) using an isocratic elution with HBS. Particle size distribution and ζ-potential were determined by dynamic light scattering at 25 °C (Zetasizer Nanoseries ZS, Malvern Instruments).

Stability of the pDNA-Loaded Liposome Suspension. The stability of the pDNA-loaded liposomes was determined by measuring the amount of pDNA for 5 h immediately after the complex formation at room temperature. This information is important in the case of storage of the liposome suspension or even during the liposome immobilization, which may take at least 4 h. Moreover, it mimics the 5 h of single dose incubation of cells with pDNA-loaded liposomes. This incubation time is a standard period of cells' transfection (*e.g.*, as with Lipofectamine) since the stimuli is added to fresh trypsinazed cells and the cells need to adhere before media change. For that, aliquots of liposome solution, formulation **F1**, and pDNA-GFP (0.4 mg/mL) were removed at each time point and the pDNA concentration was determined by the Quant-iT PicoGreen dsDNA assay kit (Invitrogen, Molecular Probes;

Oregon, USA), according to the manufacturer instructions. The fluorescence of the dye was measured at an excitation wavelength of 485/20 nm and at an emission wavelength of 528/20 nm in a microplate reader (Synergie HT, Bio-Tek; USA). The pDNA concentration for each sample was calculated using a standard curve (pDNA concentration ranging from 0.0 to 1.5 μg/mL) relating directly the pDNA quantity to the fluorescence intensity.

pDNA Loading Efficiency into Liposomes. The pDNA loading efficiency was analyzed using the formulation **F1**, by quantifying DNA and lipid content. The DNA was determined by the Quant-iT PicoGreen dsDNA assay kit, as described above. The total lipid concentration was assessed by the Bartlett colorimetric assay, as described elsewhere.[56] Briefly, the principle of the Bartlett assay is based on the colorimetric determination of inorganic phosphate. The phospholipid content of liposomes can be determined after the destruction of the phospholipids with perchloric acid to inorganic phosphate. The inorganic phosphate is converted to phospho-molybdic acid by the addition of ammonium molybdate, which is reduced to a blue colored complex by 4-amino-2-naphthyl-4-sulfonic acid during heating. This compound was determined colorimetrically at 830 nm (Synergie HT).

The ability of the liposomal vesicles to incorporate the pDNA was evaluated by calculating the system payload (PL) according to eq 1. The encapsulation efficiency (EE) was calculated as the final PL (PL_f) per initial PL (PL_i) for pDNA and HSPC according to eq 2.

$$\mathrm{PL} = \frac{\text{amount of pDNA (mol)}}{\text{amount of HSPC (mol)}} \quad (1)$$

$$\mathrm{EE}\,(\%) = \frac{\mathrm{PL_f}}{\mathrm{PL_i}} \times 100 \quad (2)$$

Immobilization of the pDNA-Loaded Liposomes at the Surface of NFMs. The immobilization of the pDNA-loaded liposomes at the surface of NFMs was performed as described in detail elsewhere.[34] Briefly, SH-functionalized electrospun PCL NFMs were immersed in 4 mL of liposome solution (formulation **F2**, 0.1 mg/mL pDNA) for 4 h.[34] Afterward, the NFMs were washed three times with 3% ethanol in phosphate buffer (pH 7.4). After pDNA-loaded liposome immobilization, the electrospun PCL NFMs were immersed in a PBS solution containing 0.5% Triton to dissolve the lipids. To determine the maximum capacity of pDNA-loaded liposome immobilized at the surface of the NFMs, the effect of washing and Triton dissolving lipid time were both studied. The experiments were performed in triplicate, and the pDNA immobilized at the surface of PCL NFMs was quantified by the Quant-iT PicoGreen dsDNA assay kit (Invitrogen, Molecular Probes; Oregon, USA) as described above. The morphology of pDNA-loaded liposomes immobilized at the surface of electrospun PCL NFM was analyzed by SEM (NanoSEM Nova 200, London). Binding of the liposomes, carrying the fluorescent dye to the SH-functionalized NFMs was analyzed by fluorescence microscopy (AXIOIMAGE RZ1M, ZEISS, Germany).

Biological Activity. *Expansion, Seeding, and Osteogenic Differentiation of Human Bone Marrow Mesenchymal Stem Cells.* hBMSCs were isolated from bone marrow aspirates collected under informed consent from patients undergoing knee arthroplasty at the Hospital de Braga, Portugal, in accordance with a protocol established between the 3B's Research Group and the Hospital de Braga approved by the ethics committee of the same hospital. Samples were collected from a 58 year old female donor, isolated, expanded, and cryopreserved until further use. hBMSCs were isolated and characterized according to the method established by Delorme and Charbord.[57] Briefly, plastic adherent fractions of marrow cells were characterized by a spindle-shaped morphology and colony-forming unit capacity; expression of surface antigens like CD 29, 73, 90, and 105, while being negative for hematopoietic markers such as CD 34 and 45 (all the antibodies were purchased from BD Pharmingen and the hBMSCs analyzed on a FACS Calibur, BD Biosciences); and by their differentiation potential into the osteogenic, chondrogenic, and adipogenic lineages. hBMSCs were expanded in basal medium consisting of MEM alpha medium (α-MEM; Gibco, GB) supplemented with 10% heat-inactivated fetal bovine serum (FBS; Gibco, GB) and 1% antibiotic/antimycotic solution (final concentration of penicillin 100 units/mL and streptomycin 100 mg/mL; Gibco, GB). Cells were cultured at 37 °C in a humidified atmosphere of 5% CO_2. Confluent hBMSCs at passage 4 were harvested for seeding onto RUNX2-loaded liposomes immobilized at the surface of electrospun PCL NFMs (*NFM+LipRUNX2*) at a density of 1×10^5 cells. Also, hBMSCs were cultured under basal medium stimulated with RUNX2-loaded liposomes in suspension (*TCPS_ LipRUNX2(susp)*), added at the same concentration of the liposomes immobilized at NFMs. The defined experimental control conditions were hBMSCs cultured onto tissue culture polystyrene (TCPS) and NFMs under basal medium (*TCPS_ Basal* and *NFM_Basal*), and under standard osteogenic differentiation medium (basal medium supplemented with 50 μg/mL ascorbic acid, 10 mM β-glycerophosphate and 10^{-7} M Dex) (*TCPS_Osteo* and *NFM_Osteo*). The constructs were retrieved at predefined culturing times, namely, 7, 14, and 21 days. All experiments were performed in triplicate and repeated twice independently.

Cell Viability and Proliferation Assessment. Cell viability for each culturing condition and time point was determined using the CellTiter 96 AQueous One Solution Cell Proliferation Assay (Promega, USA), according to the manufacturer instructions. This assay is based on the bioreduction of a tetrazolium compound, 3-(4,5-dimethylthiazol-2-yl)-5-(3-carboxymethoxyphenyl)-2-(4-sulfofenyl)-2*H*-tetrazolium [MTS], into a water-soluble brown formazan product. The absorbance was measured at 490 nm in a microplate reader (SynergieHT, Bio-Tek, USA), being related to the quantity of formazan product. Four specimens per time point were quantified.

Cell proliferation was quantified by the total amount of double-stranded DNA obtained along the culturing time. Briefly, hBMSCs within the construct were lysed by osmotic and thermal shock, and the supernatant was used for the DNA quantification assay. Quantification was performed using the Quant-iT PicoGreen dsDNA Assay kit (Invitrogen, Molecular Probes; Oregon, USA) as described above.

All data concerning cell viability, proliferation, and ALP activity was independently measured and normalized against the cell number for each sample. For that, a standard calibration curve was performed using known hBMSC cell numbers at passage 4, ranging from 0 to 5×10^5 cells, with an $n = 12$. The dsDNA concentration of these samples was determined according to the Quant-iT PicoGreen dsDNA Assay kit previously described. The following equation was obtained: $y = 0.0054x + 86.68$ with a $R^2 = 0.998$, where the y is the measured fluorescence value and the x is the cell number, and used to estimate the cell number for each individual sample based in the amount of DNA quantified.

Alkaline Phosphatase and Total Protein Quantification. The concentration of alkaline phosphatase (ALP) was determined for all time culture periods, using the same cell lysates used for DNA quantification. Briefly, the ALP quantity was assessed using the *p*-nitrophenol assay, in which 4-nitrophenyl phosphate disodium salt hexahydrate (Sigma, USA) is hydrolyzed by the intracellular ALP at the temperature of 37 °C in an alkaline buffer solution (1.5 M and pH 10.5, Sigma) to form yellow free *p*-nitrophenol. The reaction was stopped by addition of 0.3 M NaOH (Panreac Quimica, Spain) and the absorbance read at 405 nm in a microplate reader (Bio-Tek, Synergie HT, USA). Standards were prepared with 10 mM *p*-nitrophenol (pNP; Sigma, USA) solution to obtain a standard curve ranging from 0 to 250 μM. Quadruplicates of each sample and standard were made and the ALP concentrations read off from the standard curve.

For the quantification of total protein synthesized by the hBMSCs in culture, the Micro BCA Protein Assay kit (Thermo Scientific, Pierce; Rockford, USA) was used according to the manufacturer instructions. This is a colorimetric detection and quantification method which utilizes bicinchoninic acid (BCA) as the detection reagent for Cu^{1+} formed when Cu^{2+} is reduced by protein in an alkaline environment. Quadruplicates of lysed cells per culturing time were incubated at 37 °C for 2 h.

TABLE 4. List of Primer Sequences and Detailed Information

gene	primer 5′-3′	T_m (°C)	product size (bp)	seq ref (NCBI)
GAPDH	ACAGTCAGCCGCATCTTCTT	58.4	308	NM_002046.4
	GACAAGCTTCCCGTTCTCAG			
RUNX2	TTCCAGACCAGCAGCACTC	58.1	242	NM_001145920.1
	CAGCGTCAACACCATCATTC			
OCN	GTGCAGAGTCCAGCAAAGG	59.4	549	DQ007079.1
	TCAGCCACTCGTCACAGC			
OP	CCCACAGACCCTTCCAAGTA	58.4	244	AF052124.1
	GGGGACAACTGGAGTGAAAA			
ALP	CTCCTCGGAAGACACTCTG	60	238	AK312667.1
	AGACTGCGCCTGGTAGTTG			
BSP	ACTGAGCCTGTGTCTTGAAA	56.3	102	AH002985.1
	CTTCCAACAGCCAATCACTG			

A purple-colored reaction product was measured at 562 nm in a microplate reader (SynergieHT, Bio-Tek, USA) and calculated based on an albumin standard curve, ranging from 0 to 40 μg/mL.

RNA Isolation and Real-Time Quantitative Polymerase Chain Reaction. At each culturing time, the hBMSCs were washed with PBS, immersed in Tri reagent (Sigma-Aldrich, USA), and stored at −80 °C until further use. Proteins were removed with chloroform/isoamylalcohol (BioChemica, AppliChem; Germany) extraction, and the RNA pellets were washed once with 2-propanol (Sigma-Aldrich; USA) and once with 70% ethanol (Panreac; Spain). The total RNA pellets were reconstituted in RNase-free water (Gibco, Invitrogen; UK). Determination of the RNA concentration for each replica (quadruplicates of each condition per time point) was performed by micro-spectrophotometry (NanoDrop 1000, Thermo Scientific; USA).

Reverse transcriptase (RT)-PCR was performed according to the protocol from iScript cDNA synthesis kit (Quanta BioSciences; Gaithersburg, MD). Briefly, a reaction mixture consisting of 1X iScript reaction mix, 1 μL of iScript reverse transcriptase, 100 ng of RNA template, and nuclease-free water was prepared in 20 μL of total volume. The single-strand cDNA synthesis occurred by incubating the complete reaction mixture for 5 min at 22 °C, followed by 30 min at 42 °C, and terminated by an incubation at 85 °C for 5 min.

Amplification of the target cDNA for RT-PCR quantification was performed according to manufacturer, using 1 μL of RT cDNA products, 250 nM each primer (bone-specific primer sets listed in ref 33) 1X PerfeCta SYBR Green FasterMix (Quanta BioSciences; Gaithersburg, MD) and nuclease-free water, in a final volume of 20 μL. Forty-five cycles of denaturation (95 °C, 10 s), annealing (temperature-dependent on the gene; Table 4; 30 s), and extension (72 °C, 30 s) were carried out in the Mastercycler epgradient S realplex thermocycler (Eppendorf; Hamburg, Germany) for all genes. The transcript expression data were normalized to the housekeeping gene *glyceraldehydes-3-phosphate-dehygrogenase* (*GAPDH*) and the quantification performed according to the Livak method ($2^{-\Delta\Delta CT}$ method), considering the basal medium conditions (*TCPS_Basal* and *NFM_Basal*) for each time point as calibrator.

Statistical Analysis. Data were statistically analyzed using IBM SPSS software (version 20; SPSS Inc.). We first applied the Shapiro-Wilk test to test the assumption of normality, and the results showed that the data were not following a normal distribution. Consequently, the non-parametric Mann−Whitney U and Kruskal−Wallis tests were applied. The *p* values less than 0.01 were considered statistically significant in the analysis of the results.

Conflict of Interest: The authors declare no competing financial interest.

Acknowledgment. The authors thank the Portuguese Foundation for Science and Technology for the PhD grant of N.M. (SFRH/BD/62465/2009), and the Post-Doc grants of A.M. (SFRH/BPD/70669/2010), and the OsteoGraphy project (PTDC/EME-MFE/2008). This work was partly supported by the POLARIS (FP7-REGPOT-2012-2013-1), MaxBone (PTDC/SAU-ENB/115179/2009), and RL3-TECT-NORTE-01-0124-FEDER-000020, co-financed by North Portugal Regional Operational Programme (ON.2 − O Novo Norte), under the National Strategic Reference Framework (NSRF), through the European Regional Development Fund (ERDF) projects.

REFERENCES AND NOTES

1. Giannoudis, P. V.; Dinopoulos, H.; Tsiridis, E. Bone Substitutes: An Update. *Injury* **2005**, *36 Suppl 3*, S20–S27.
2. Damien, C. J.; Parsons, J. R. Bone-Graft and Bone-Graft Substitutes: A Review of Current Technology and Applications. *J. Appl. Biomater.* **1991**, *2*, 187–208.
3. Winn, S. R.; Chen, J. C.; Gong, X.; Bartholomew, S. V.; Shreenivas, S.; Ozaki, W. Non-viral-Mediated Gene Therapy Approaches for Bone Repair. *Orthod. Craniofac. Res.* **2005**, *8*, 183–190.
4. Santo, V. E.; Sato, K.; Ratanavaraporn, J.; Gomes, M. E.; Mano, J. F.; Reis, R. L.; Tabata, Y. Enhanced Orthotopic Bone Regeneration Promoted by Intracellular Delivery of Dexamethasone. *J. Tissue Eng. Regener. Med.* **2012**, *6*, 330–330.
5. Hutmacher, D. W.; Schantz, J. T.; Lam, C. X. F.; Tan, K. C.; Lim, T. C. State of the Art and Future Directions of Scaffold-Based Bone Engineering from a Biomaterials Perspective. *J. Tissue Eng. Regener. Med.* **2007**, *1*, 245–260.
6. Martins, A.; Duarte, A. R. C.; Faria, S.; Marques, A. P.; Reis, R. L.; Neves, N. M. Osteogenic Induction of hBMSCs by Electrospun Scaffolds with Dexamethasone Release Functionality. *Biomaterials* **2010**, *31*, 5875–5885.
7. Martins, A.; Chung, S.; Pedro, A. J.; Sousa, R. A.; Marques, A. P.; Reis, R. L.; Neves, N. M. Hierarchical Starch-Based Fibrous Scaffold for Bone Tissue Engineering Applications. *J. Tissue Eng. Regener. Med.* **2009**, *3*, 37–42.
8. Nair, L. S.; Laurencin, C. T. Nanofibers and Nanoparticles for Orthopaedic Surgery Applications. *J. Bone Jt. Surg., Am. Vol.* **2008**, *90* (Supplement_1), 128–131.
9. Rujitanaroj, P.-O.; Wang, Y.-C.; Wang, J.; Chew, S. Y. Nanofiber-Mediated Controlled Release of siRNA Complexes for Long Term Gene-Silencing Applications. *Biomaterials* **2011**, *32*, 5915–5923.
10. Uyar, T.; Havelund, R.; Hacaloglu, J.; Besenbacher, F.; Kingshott, P. Functional Electrospun Polystyrene Nanofibers Incorporating α-, β-, and γ-Cyclodextrins: Comparison of Molecular Filter Performance. *ACS Nano* **2010**, *4*, 5121–5130.
11. Vo, T. N.; Kasper, F. K.; Mikos, A. G. Strategies for Controlled Delivery of Growth Factors and Cells for Bone Regeneration. *Adv. Drug Delivery Rev.* **2012**, *64*, 1292–1309.
12. Von Groll, A.; Levin, Y.; Barbosa, M. C.; Ravazzolo, A. P. Linear DNA Low Efficiency Transfection by Liposome Can Be Improved by the Use of Cationic Lipid as Charge Neutralizer. *Biotechnol. Prog.* **2006**, *22*, 1220–1224.
13. Gomes-da-Silva, L. C.; Santos, A. O.; Bimbo, L. M.; Moura, V.; Ramalho, J. S.; de Lima, M. C. P.; Simoes, S.; Moreira, J. N. Toward a siRNA-Containing Nanoparticle Targeted to Breast Cancer Cells and the Tumor Microenvironment. *Int. J. Pharm.* **2012**, *434*, 9–19.
14. Jang, J. H.; Houchin, T. L.; Shea, L. D. Gene Delivery from Polymer Scaffolds for Tissue Engineering. *Expert Rev. Med. Devices* **2004**, *1*, 127–138.
15. Pornpattananangkul, D.; Olson, S.; Aryal, S.; Sartor, M.; Huang, C.-M.; Vecchio, K.; Zhang, L. Stimuli-Responsive Liposome Fusion Mediated by Gold Nanoparticles. *ACS Nano* **2010**, *4*, 1935–1942.
16. Storrie, H.; Mooney, D. J. Sustained Delivery of Plasmid DNA from Polymeric Scaffolds for Tissue Engineering. *Adv. Drug Delivery Rev.* **2006**, *58*, 500–514.
17. Kulkarni, M.; Greiser, U.; O'Brien, T.; Pandit, A. Liposomal Gene Delivery Mediated by Tissue-Engineered Scaffolds. *Trends Biotechnol.* **2010**, *28*, 28–36.
18. Woodle, M. C.; Scaria, P. Cationic Liposomes and Nucleic Acids. *Curr. Opin. Colloid Interface Sci.* **2001**, *6*, 78–84.

19. Obata, Y.; Saito, S.; Takeda, N.; Takeoka, S. Plasmid DNA-Encapsulating Liposomes: Effect of a Spacer between the Cationic Head Group and Hydrophobic Moieties of the Lipids on Gene Expression Efficiency. *Biochim. Biophys. Acta, Biomembr.* **2009**, *1788*, 1148–1158.
20. Monteiro, N.; Martins, A.; Ribeiro, D.; Faria, S.; Fonseca, N. A.; Moreira, J. N.; Reis, R. L.; Neves, N. M. On the Use of Dexamethasone-Loaded Liposomes to Induce the Osteogenic Differentiation of Human Mesenchymal Stem Cells. *J. Tissue Eng. Regener. Med.* **2013**, DOI: 10.1002/term.1817.
21. Yau, W. W. Y.; Rujitanaroj, P.-O.; Lam, L.; Chew, S. Y. Directing Stem Cell Fate by Controlled RNA Interference. *Biomaterials* **2012**, *33*, 2608–2628.
22. Bianco, P.; Riminucci, M.; Gronthos, S.; Robey, P. G. Bone Marrow Stromal Stem Cells: Nature, Biology, and Potential Applications. *Stem Cells* **2001**, *19*, 180–192.
23. Chamberlain, G.; Fox, J.; Ashton, B.; Middleton, J. Concise Review: Mesenchymal Stem Cells: Their Phenotype, Differentiation Capacity, Immunological Features, and Potential for Homing. *Stem Cells* **2007**, *25*, 2739–2749.
24. Pittenger, M. F.; Mackay, A. M.; Beck, S. C.; Jaiswal, R. K.; Douglas, R.; Mosca, J. D.; Moorman, M. A.; Simonetti, D. W.; Craig, S.; Marshak, D. R. Multilineage Potential of Adult Human Mesenchymal Stem Cells. *Science* **1999**, *284*, 143–147.
25. Maia, J.; Santos, T.; Aday, S.; Agasse, F.; Cortes, L.; Malva, J. O.; Bernardino, L.; Ferreira, L. Controlling the Neuronal Differentiation of Stem Cells by the Intracellular Delivery of Retinoic Acid-Loaded Nanoparticles. *ACS Nano* **2011**, *5*, 97–106.
26. Caplan, A. I. Adult Mesenchymal Stem Cells for Tissue Engineering *versus* Regenerative Medicine. *J. Cell. Physiol.* **2007**, *213*, 341–347.
27. Lennon, D. P.; Haynesworth, S. E.; Bruder, S. P.; Jaiswal, N.; Caplan, A. I. Human and Animal Mesenchymal Progenitor Cells from Bone Marrow: Identification of Serum for Optimal Selection and Proliferation. *In Vitro Cell. Dev. Biol.* **1996**, *32*, 602–611.
28. Moutsatsos, I. K.; Turgeman, G.; Zhou, S. H.; Kurkalli, B. G.; Pelled, G.; Tzur, L.; Kelley, P.; Stumm, N.; Mi, S.; Muller, R.; Zilberman, Y.; Gazit, D. Exogenously Regulated Stem Cell-Mediated Gene Therapy for Bone Regeneration. *Mol. Ther.* **2001**, *3*, 449–461.
29. Kular, J.; Tickner, J.; Chim, S. M.; Xu, J. An Overview of the Regulation of Bone Remodelling at the Cellular Level. *Clin. Biochem.* **2012**, *45*, 863–873.
30. Kirkham, G. R.; Cartmell, S. H. Genes and Proteins Involved in the Regulation of Osteogenesis. In *Topics in Tissue Engineering*; University of Oulu: Finland, 2007; Vol. 3.
31. Komori, T. Regulation of Osteoblast Differentiation by Transcription Factors. *J. Cell. Biochem.* **2006**, *99*, 1233–1239.
32. Nakashima, K.; de Crombrugghe, B. Transcriptional Mechanisms in Osteoblast Differentiation and Bone Formation. *Trends Genet.* **2003**, *19*, 458–466.
33. Yoshida, C. A.; Furuichi, T.; Fujita, T.; Fukuyama, R.; Kanatani, N.; Kobayashi, S.; Satake, M.; Takada, K.; Komori, T. Core-Binding Factor Beta Interacts with RUNX2 and Is Required for Skeletal Development. *Nat. Genet.* **2002**, *32*, 633–638.
34. Monteiro, N.; Martins, A.; Pires, R. A.; Faria, S.; Fonseca, N. A.; Moreira, J. N.; Reis, R. L.; Neves, N. M. Immobilization of Bioactive Factor-Loaded Liposomes at the Surface of Electrospun Nanofibers Targeting Tissue Engineering. *Biomater Sci.* **2014**, *2*, 1195–1209.
35. Jaaskelainen, I.; Monkkonen, J.; Urtti, A. Oligonucleotide-Cationic Liposome Interactions. A Physicochemical Study. *Biochim. Biophys. Acta, Biomembr.* **1994**, *1195*, 115–123.
36. Tros de Ilarduya, C.; Sun, Y.; Duezguenes, N. Gene Delivery by Lipoplexes and Polyplexes. *Eur. J. Pharm. Sci.* **2010**, *40*, 159–170.
37. Jeffs, L. B.; Palmer, L. R.; Ambegia, E. G.; Giesbrecht, C.; Ewanick, S.; MacLachlan, I. A Scalable, Extrusion-Free Method for Efficient Liposomal Encapsulation of Plasmid DNA. *Pharm. Res.* **2005**, *22*, 362–372.
38. Schlick, T.; Li, B.; Olson, W. K. The influence of Salt on the Structure and Energetics of Supercoiled DNA. *Biophys. J.* **1994**, *67*, 2146–2166.
39. Bailey, A. L.; Cullis, P. R. Modulation of Membrane-Fusion by Asymmetric Transbilayer Distributions of Amino Lipids. *Biochemistry (Moscow)* **1994**, *33*, 12573–12580.
40. Semple, S. C.; Klimuk, S. K.; Harasym, T. O.; Dos Santos, N.; Ansell, S. M.; Wong, K. F.; Maurer, N.; Stark, H.; Cullis, P. R.; Hope, M. J.; Scherrer, P. Efficient Encapsulation of Antisense Oligonucleotides in Lipid Vesicles Using Ionizable Aminolipids: Formation of Novel Small Multilamellar Vesicle Structures. *Biochim. Biophys. Acta, Biomembr.* **2001**, *1510*, 152–166.
41. Xu, Y.; Hui, S.-W.; Frederik, P.; Szoka, F. C., Jr. Physicochemical Characterization and Purification of Cationic Lipoplexes. *Biophys. J.* **1999**, *77*, 341–353.
42. Hristova, K.; Kenworthy, A.; McIntosh, T. J. Effect of Bilayer Composition on the Phase Behavior of Liposomal Suspensions Containing Poly(ethylene glycol)-Lipids. *Macromolecules* **1995**, *28*, 7693–7699.
43. Adler, A. F.; Leong, K. W. Emerging Links between Surface Nanotechnology and Endocytosis: Impact on Nonviral Gene Delivery. *Nano Today* **2010**, *5*, 553–569.
44. Zhang, Y.; Deng, X.; Scheller, E. L.; Kwon, T.-G.; Lahann, J.; Franceschi, R. T.; Krebsbach, P. H. The Effects of RUNX2 Immobilization on Poly(ε-caprolactone) on Osteoblast Differentiation of Bone Marrow Stromal Cells *in Vitro*. *Biomaterials* **2010**, *31*, 3231–3236.
45. Yoshikawa, T.; Uchimura, E.; Kishi, M.; Funeriu, D. P.; Miyake, M.; Miyake, J. Transfection Microarray of Human Mesenchymal Stem Cells and On-Chip siRNA Gene Knockdown. *J. Controlled Release* **2004**, *96*, 227–232.
46. Bengali, Z.; Pannier, A. K.; Segura, T.; Anderson, B. C.; Jang, J.-H.; Mustoe, T. A.; Shea, L. D. Gene Delivery through Cell Culture Substrate Adsorbed DNA Complexes. *Biotechnol. Bioeng.* **2005**, *90*, 290–302.
47. Yang, S. Y.; Wei, D. Y.; Wang, D.; Phimphilai, M.; Krebsbach, P. H.; Franceschi, R. T. *In Vitro* and *In Vivo* Synergistic Interactions between the RUNX2/Cbfa1 Transcription Factor and Bone Morphogenetic Protein-2 in Stimulating Osteoblast Differentiation. *J. Bone Miner. Res.* **2003**, *18*, 705–715.
48. Okazaki, A.; Jo, J. I.; Tabata, Y. A Reverse Transfection Technology To Genetically Engineer Adult Stem Cells. *Tissue Eng.* **2007**, *13*, 245–251.
49. Bellows, C. G.; Aubin, J. E.; Heersche, J. N. M. Initiation and Progression of Mineralization of Bone Nodules Formed *in Vitro*—The Role of Alkaline-Phosphatase and Organic Phosphate. *Bone Miner.* **1991**, *14*, 27–40.
50. Hoemann, C. D.; El-Gabalawy, H.; McKee, M. D. *In Vitro* Osteogenesis Assays: Influence of the Primary Cell Source on Alkaline Phosphatase Activity and Mineralization. *Pathol. Biol.* **2009**, *57*, 318–323.
51. Schroeder, T. M.; Jensen, E. D.; Westendorf, J. J. RUNX2: A Master Organizer of Gene Transcription in Developing and Maturing Osteoblasts. *Birth Defects Res., Part C* **2005**, *75*, 213–225.
52. Komori, T. Signaling Networks in RUNX2-Dependent Bone Development. *J. Cell. Biochem.* **2011**, *112*, 750–755.
53. Han, D.; Li, J. J. Repair of Bone Defect by Using Vascular Bundle Implantation Combined with RUNX II Gene-Transfected Adipose-Derived Stem Cells and a Biodegradable Matrix. *Cell Tissue Res.* **2013**, *352*, 561–571.
54. Makita, N.; Suzuki, M.; Asami, S.; Takahata, R.; Kohzaki, D.; Kobayashi, S.; Hakamazuka, T.; Hozumi, N. Two of Four Alternatively Spliced Isoforms of RUNX2 Control Osteocalcin Gene Expression in Human Osteoblast Cells. *Gene* **2008**, *413*, 8–17.
55. Tyllianakis, P.; Kakabakos, S.; Evangelatos, G.; Ithakissios, D. Colorimetric Determination of Reactive Primary Amino Groups of Macro- and Microsolid Supports. *Appl. Biochem. Biotechnol.* **1993**, *38*, 15–25.
56. Torchilin, V. P.; Weissig, V. *Liposomes: A Practical Approach*, 2nd ed.; Oxford University Press: New York, 2003.
57. Delorme, B.; Charbord, P. Culture and Characterization of Human Bone Marrow Mesenchymal Stem Cells. *Methods Mol. Med.* **2007**, *140*, 67–81.